

Improving the iterative back projection estimation through Lorentzian sharp infinite symmetrical filter

Amir Nazren Abdul Rahim^{1,2}, Shahrul Nizam Yaakob^{1,2}, Lee Yeng Seng¹, Mohd Wafi Nasrudin^{1,2}, Iszaidy Ismail^{1,2}

¹Faculty of Electronic Engineering Technology, Universiti Malaysia Perlis, Padang Besar, Perlis, Malaysia

²Centre of Excellence Advanced Computing, Universiti Malaysia Perlis, Arau, Perlis, Malaysia

Article Info

Article history:

Received Oct 13, 2020

Revised Jan 3, 2022

Accepted Jan 28, 2022

Keywords:

Enhancement

Image processing

Iterative back projection

Ringing effect

Super resolution

ABSTRACT

This study proposed an enhancement technique for improvising the estimation technique in iterative back projection (IBP) by using the Lorentzian error function with a sharp infinite symmetrical filter (SISEF). The IBP estimation is an iteratively based error correction that can minimize the error reconstruction significantly. However, the IBP has a drawback in that it suffers from jaggy and ringing artifacts as a result of the iterative reconstruction method and the absence of edge guidance. Furthermore, because the IBP estimator tended to oscillate at the same solution frequently, numerous iterations were required. Therefore, this study proposed edge enhancement to enhance the estimator by using the combination of the IBP with Lorentzian SISEF to produce a finer high-resolution output image. As a result, the SISEF is used to improvise the estimator by providing high accuracy of edge detail information for enhancing the edge image. At the same time, the Lorentzian error norm helps to increase the robustness of the IBP algorithm from contamination of additional noise and the ringing artifacts.

This is an open access article under the [CC BY-SA](https://creativecommons.org/licenses/by-sa/4.0/) license.



Corresponding Author:

Amir Nazren Bin Abdul Rahim

Faculty of Electronic Engineering Technology, Universiti Malaysia Perlis

Level 1, Building S2, UniCITI Alam Campus, Sungai Chuchuh, 02100 Padang Besar, Perlis, Malaysia

Email: amirnazren@unimap.edu.my

1. INTRODUCTION

Most digital imaging applications demand higher-quality image acquisition. The finer quality of the image or high resolution (HR) image is crucial to gain the most useful information as much possible [1]–[17]. However, in the reality of image acquisition system was introduced a degraded quality of the output image or low resolution (LR) image by the hardware limitation. This low-quality image was degraded by many factors contributed including internal and external environments. For instance, a finite number of resolution acquisition sensors may draw limited information on the digital image. Moreover, the motion blur appeared on the image when the poor handling of the acquisition device between the scenes. Besides that, the acquisition system may introduce a noisy image due to limitations of the sensor's device and additional signals during the transmission medium [18]–[33]. However, the hardware improvement not always reliable in most cases. It because the improvement of the sensor acquisition system would lead to a large expenditure budget, and unreliable for real applications. Thus, image recovery through the super resolution technique is the best choice to produce a finer quality image with enlarge the image size capability.

This study is intended to highlight the constraints on the super resolution (SR) technique and provide some improvements to improve the SR. The essential in SR is the reconstruction technique, which is based on the manipulation of the global imaging problem model. This model is generated based on the

existence of several limitation factors in the real acquisition system such as constraints that occurred in the point spread function (PSF) of the camera that contains information of blur, translation, and decimation factors [34]. In addition, some constraints on the image acquisition may lead to the presence of global noise that contaminated the acquired image [21]–[23], [26], [29]–[33]. The SR reconstruction is referring to the recovery techniques in image processing that obtains a high resolution (HR) image from observed single or multiple LR images. To produce the HR image, the researcher has manipulated the mathematical expression of the imaging model which describes the sensor characteristics, such as motion blur, decimation, and shifted translation in the camera PSF [1], [2], [10], [11], [15].

The SR reconstruction method consists of three basic tasks: registration, interpolation, and restoration [35]. This task can be implemented separately or simultaneously which depends on how the technique is adopted. The re-construction process takes sub-pixel shifted information from the sequence of LR images or sensor parameters provided by the image registration task. Indeed, the accuracy of sub-pixel motion is a very important factor for SR reconstruction solution to produce a finer image [21], [23], [27], [31], [34], [36]–[47]. Then, the interpolation task is taking place to align the nonuniform space of the LR image onto a uniformly HR image grid. Finally, the reconstruction task deploys to restore the finer HR image by removing the blur and noise effects.

The iterative back projection (IBP) is among the first spatial-based SR reconstruction. This technique is formulated by Irani and Peleg [41], [46], [48], this approach is similar to the reconstruction of 2-D objects from 1-D projections in computer-aided tomography (CAT). Each of the LR image resolution pixels is a projection of a region in the scene whose size is determined by the imaging blur. Then high resolution is determined using a similar back-projection method in CAT. The technique is equipped with sub-pixel accuracy as image registration to align the LR images on the HR grid before increases the size image resolution. Then, the HR image is estimated by back projecting the error between simulated LR images and observed LR images. The gradient or error is determined the same as the least square error in l_2 norm computation. Moreover, the IBP technique requires an initial guess for very first-timer estimation. If the initial guess estimated is close to the optimal point in the search space, then the estimation will converge smoothly.

This back-projection technique can minimize the error of reconstruction efficiently in an iterative manner. To correct the next estimated image, this error reconstruction is back-projected to the HR grid. However, by removing the blur effect, this technique can improve the image intensity [24], [33], [49]–[52]. The iterative procedure, on the other hand, contains defects that cause ringing artifacts at the edges. This condition emerges as a result of incorrect back projecting due to the lack of edge guidance during projection [22], [33], [49], [53]–[57]. Therefore, this study proposed the improvement with the edge enhancement technique embedded with the IBP reconstruction technique by using a combination of the Lorentzian function and sharp infinite symmetrical exponential filter (LSISEF). The SISEF function has high localization edge detection and it is used to preserve the possible edge detected. Coincide, supplies the edge guidance during the back projecting to avoid across edge projection, thus the ringing effects be reduced. Besides that, the Lorentzian error norm is deployed to suppress the amount of error in the cost function. As a result, the suggested methodology can improve HR estimation by maintaining lost frequency information while being resistant to ringing effects and extra noise [32], [58]–[60].

2. SUPER RESOLUTION

Since the conventional super resolution (SR) approach suffers from HR estimate imperfections. This study gets a lot of attention from the researcher to produce a better technique for improving the ordinary one. Therefore, Chiang and Boulton [61] proposed that the resampling algorithm be improved by incorporating the image warping methodology into the IBP reconstruction. It was accomplished by combining the imaging system's degradation model with integrating resampled data, which resulted in a more accurate estimation of IBP. Cohen and Dinstein [62] indicated that the final image resolution might be improved by using a polyphase filter to replace the geometric transformation inside the IBP algorithm. Furthermore, Kim *et al.* [63] suggested an edge enhancement strategy that uses anisotropic diffusion to minimize noise and highlight edges. To remove blur efficiently, Bose *et al.* [64] proposed optimal regularization using L-Curve for handling the degraded image. To provide a better reconstruction technique, Rajan and Chaudhuri [65] used generalized interpolation scheme development for image resizing and proposed a combination magnetic resonance fingerprinting (MRF) and MAP estimator for SR reconstruction. Sun *et al.* [66] improved the quality hallucinate image by implementing Markov-chain based inference algorithm inside back-projection. Rajan and Chaudhuri [67] proposed super-resolution reconstruction using a machine learning (ML) estimator with MRF regularization to estimate the depth map and focus on the scene image.

Furthermore, the resolution improvement via implementing the 3D motion is estimated recursively in an extended Kalman filter and by a novel image warping procedure [68]. The IBP reconstruction error can be reduced by incorporating adaptively nonlocal back projection [69]. To improve the reconstruction errors reconstruction in the IBP, Dong *et al.* [70] proposed the non-local IBP algorithm in which the enlargement process incorporates adaptively the non-local information. The resolution improvement in efficient highlight edges image can be done by embedding the un-sharpening mask by using the SRUM algorithm [71]. Furthermore, Yan *et al.* [72] proposed a combination Papoulis-Gerchberg extrapolation inside the IBP to enhance the spiral CT slice image. Furthermore, the IBP technique's efficiency is improved by using a wavelet locally adaptive approach to estimate the first initial guess rather than the traditional interpolation approach [73]. Following that, Liang and Gan [74] show that using the non-local IBP fast technique, they can improve edge identification during the initial interpolated image. Besides that, the L^*a*b domain was proposed by Bengtsson *et al.* [75] for improving the human visual system in the HR image. By maintaining the edge information details, the output HR image will be improved.

Besides that, to recover a high-resolution image, Bareja and Modi [76] proposed combining the IBP technique with the canny edge detector to reconstruct a high-resolution image. As a result, the error difference between degraded and estimated images is used to recover lost frequency. Moreover, the proposed hybrid technique was introduced between the IBP technique with the Cuckoo optimizer by improving the initial guess and HR output image [77]. Rasti *et al.* [78] proposed an approach via using the interpolation method on the LR before registered inside the IBP algorithm. Cheref and Yousfi [25] used the anisotropic diffusion approach to preserve possible edge pictures. In SR reconstruction, Maiseli *et al.* [79] used adaptive Perona Malik as edge preservation.

This work continued with improving the IBP result by reducing the ringing effects by applied variant and local variance variant based on adaptive analysis [80]. The visual quality image improved while applied the sparse linear regression and iterative back projection. Additionally, they modified the Gaussian high pass filter to refining the initial guess [81]. When the residual error was reduced by utilizing anisotropic diffusion to assist the IBP estimator in producing a sharper HR image with edge preservation, the accuracy of the reconstruction was improve. Hassen and Jahmeerbacus [82] proposed combining the IBP with a Canny edge detector and a Gabor filter to improve back-projection error minimization. Furthermore, Nayak and Patra [83] proposed using the P-Spline and MuCSO-QPSO algorithms to improve the edge image of the IBP methodology, with the P-Spline providing crisp edge information and MuCSO-QPSO optimizing the estimation approach.

In work [84], a simultaneous task in SR reconstruction is introduced for robust outliers and preserving the edge image by implementing the Huber norm for robust regularization. Meanwhile, in [83], [85] the proposed a robust iterative super resolution reconstruction by using Lorentzian Thikonov with a Bayesian MAP estimator. This technique is used to remove multi kinds of artifacts and improved the estimation [83], [85]. The IBP algorithm also suffers from ringing effects. This problem can be reduced after employing total variation as a penalty function during the reconstruction process [86]. The study for removing the noise and ringing effects is continued in work [87], through employing an effective edge-guided interpolation method with a bilateral filter for significantly removed the artifacts. The regularization method proposed by Feng and Lei [88] is a combination of the total generalized variation (TGV) and Shearlet Transform to eliminate the artifacts and preserve the edges of the image. To suppress the ringing artifacts in the IBP output, Yang *et al.* [89] introduced a variation and local variance variation based on an adaptive inside the reconstruction. Many proposed algorithms have shown improvements in the robustness towards outliers and noise. However, the improvements should bring benefits to the SR quality image and the computational complexity as well.

3. METHOD

3.1. Imaging model

This section is discussed the PSF model of the SR reconstruction method. The digital application represents an image in matrix form as a column-wise lexicographically order matrix notation. Which the input is given a number N observed of LR images $\{Y_k\}_{k=1}^N$, where each of the input images has matrix size $[M_k \times M_k]$. Then the reconstruction output HR image X has matrix size $[L \times L]$, where commonly the size $L > M_k$ and $L = \alpha M_k$ the α is a multiplication enlargement factor. Since each of the observed input image has arbitrary geometric warping, linear space-variant blurring, and uniform rational decimating done on the ideal HR image X . Furthermore, the input images assumed each of them are degraded by non-homogeneous additive noise. Thus, all parameters involved above description to an analytical model show as in (1):

$$Y_k = D_k B_k W_k X + \eta_k \quad (1)$$

where, W_k is $[L^2 \times L^2]$ the matrix representing geometric warping performed on the image X . Then, B_k is the linear space-variant blur matrix of size $[L^2 \times L^2]$ and D_k is a $[M^2 \times L^2]$ matrix size represents as a decimation operator. Where η_k stands for the additive noise in the k th measurement with the positive definite autocorrelation matrix with matrix size $[M_k \times M_k]$. During the experiment setup, all matrices (D_k, B_k, T_k, η_k) are assumed to be known in advance after preparing by the prerequisite image registration stage.

The parameter matrix D_k represents the decimation factor, which this ratio factor represents an enlargement factor size between the ideal reference image and the k th measurement image. This ratio is obtained from the division between the size of a pixel in the measured image M_k^2 and the reference image L^2 . If choosing a very high ratio factor of the decimation and will cause the ill-posed problem and the image suffers from lost a lot of information.

3.2. Iterative back projection

The IBP technique's fundamental idea is to reconstruct the HR image from several degraded input images that have been detected. The difference between simulated and observed LR pictures is projected back to estimate the difference. The estimating method is repeated until the HR picture generates the same LR images as observed LR images after passing through the same blurring and downsampling method. The IBP method can divide into two phases are simulates the observed image and back projection the error to reconstruct the HR estimation [46]. The first phase is the algorithm has to construct the simulated LR images Y_k .

$$Y_k = D_k B_k W_k X \quad (2)$$

By referring to (2), the observed LR image known as Y with the number k^{th} of images. While the production of pixel intensity of LR images is influenced by the degradation function derived from the HR image X . This degradation function kernel is the yield a combination of the blur kernel function B_k and translation wrapping function W_k before downsampling by the decimation operator D .

Initially, the IBP technique procedures starting with deploys an average method to compute the initial guess $X^{(0)}$ HR image. The next stage is the imaging process produces the set of simulated LR images which are known as $Y_k^{(0)}$. However, initial guessing may result in multiple solutions rather than a single correct solution. The algorithm's ability to discover a unique, quicker, and smooth answer is dependent on the accuracy of the first estimate technique. Recently, the average of the observed registered LR images, as shown in (3), is a good initial guess method [46].

$$X^{(0)} = \frac{1}{N} \sum_{k=1}^N W_k^{-1}(Y_k) \quad (3)$$

When the initial guess HR image $X^{(0)}$ is equal with the reference image, thus the simulated images $Y_k^0 = D_k B_k W_k X^{(0)}$ should be matching with the observed images Y_k and no further correction is needed. If the between Y_k and Y_k^0 still not identical then, by back projecting the error and combining the current information in the HR grid, the initial guess is improved even further. This step of the process is yielding a better result to the next HR image $X^{(1)}$ such as in (4):

$$f^{t+1} = f^t + \frac{1}{N} \sum_{k=1}^N Q_k^T [Y_k - Q_k f^t] \quad (4)$$

where

$$Q_k = D_k B_k W_k \quad (5)$$

This procedure keeps repeating iteratively until the error is minimized enough. The error function can be described as (6).

$$e^t = \sqrt{\frac{1}{N} \sum_{k=1}^N \|Y_k - Y_k^t\|_2^2} \quad (6)$$

3.3. Infinite symmetrical exponential filter (isef)

The Shen Castan edge detector or infinite symmetrical exponential filter (ISEF) is an ideal smoothing filter with a relatively simple recursive method [90]. The implementation of the differentiation optimal exponential in discrete form is the heart of this filter. It has a positive impact on identifying the edge

picture since it responds less to noise and has a high degree of precision in edge localization. Edge detection was proposed using the maxima of gradient (GEF) or the zeros crossing of the second directional derivative along the gradient direction (SDEF). When it comes to edge detection, the Laplacian Gaussian filter confronts a tradeoff between noise insensibility and precise localization.

To overcome this challenge, the ISEF created a linear filter based on a one-step model and multi-edge detection. This optimal smoothing filter is an asymmetric exponential filter with a very simple recursive algorithm for infinitely large window sizes. The difference between the input and output of this recursive filter, which is capable of detecting edges with low noise sensitivity and high localization precision [90]. For symmetric exponential filters, the ISEF filter generates the GEF and SDEF from the first and second derivatives of the operator. The (7) is the normalized symmetric exponential filter in one dimension:

$$f_L(x) = C(f_1(x) + f_2(x) - a_0\delta(x)) \tag{7}$$

where

$$C = \frac{1}{(2-a_0)} \tag{8}$$

The exponential is the asymmetrical function which can be distinguished into the right side function $f_1(x)$ and the left side function $f_2(x)$. Thus, the second derivative of exponential function for the SDEF along the x-axis can describe in (9):

$$I_{xx}(x, y) = \frac{\partial^2}{\partial x^2}(I(x, y) * f(x, y)) \tag{9}$$

where, in the discrete form of the SDEF shown in (10):

$$I_{xx}(x, y) = I(x, y) * f_1(y) * f_2(y) * (f_1(y) + (y)) - 2(I(x, y) * f_1(y) * f_2(y)) \tag{10}$$

The equation above also can be duplicated for calculating the gradient along the y axis direction. For instance, this equation flows can be illustrated in the process flow in Figure 1.

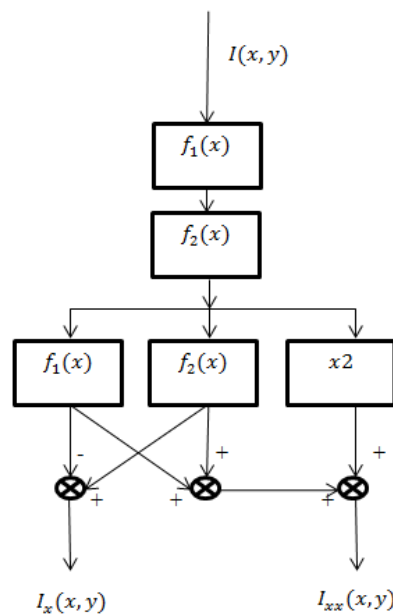


Figure 1. ISEF process flow

3.4. Lorentzian function

The noise outliers can reduce by deploying a robust error norm in the estimation stage. Then, the Lorentzian error norm is deployed to handle this constraint. This error norm which detected by Lorentzian

then projecting back those errors between an estimated HR image with observed LR images on the next HR estimation process [91]–[93]. Based on this characteristic, thus the Patanavijit proposed the estimation SR reconstruction using combination with the Lorentzian error norm. Where the ρ_{LOR} is the Lorentzian error norm function and this parameter value compute in pixel-wise operation such in (11):

$$\rho_{LOR}(x) = \log \left[1 + \frac{1}{2} \left(\frac{x}{T} \right)^2 \right] \tag{11}$$

where, the T is the Lorentzian constant parameter also known as the soft threshold value. When the value $x < T$ then the function obeys the norm L2 form, but the result be saturated when inverse condition, where ψ_{LOR} is known as the Lorentzian norm influence function. The Lorentzian error norm function and Lorentzian influence function are illustrated in Figure 2(a) and Figure 2(b) respectively.

$$\psi_{LOR}(x) = \frac{2x}{2T^2+x^2} \tag{12}$$

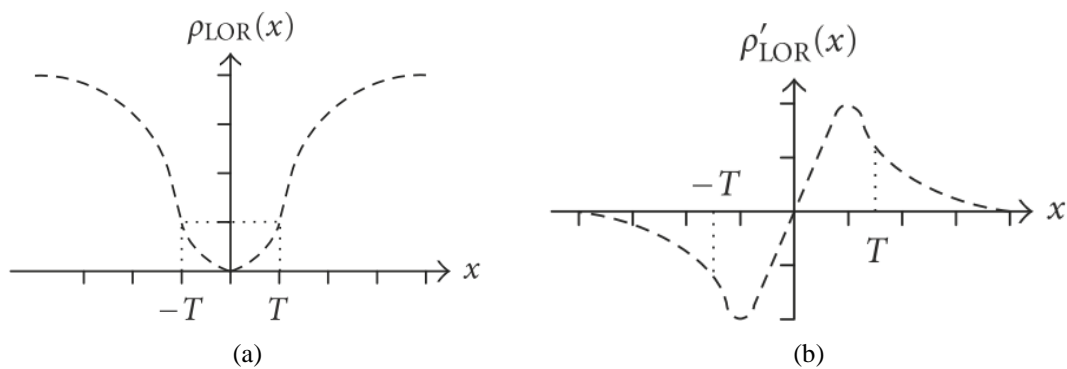


Figure 2. Lorentzian response (a) Lorentzian error norm and (b) influence function [83]

3.5. Propose ibp technique with lorentzian sharp isef regulator

The performance of the edge enhancement technique depends on the accuracy of the edge detector. The finest edge detector could offer high precision localization, a small error rate, and only detect the real edges. This study realizes the ISEF gives a promising accuracy during edge detection. This filter uses an exponential function based on designing the filter. Whereas this filter provides better edge detection than the filter Gaussian based. This study prefers to use the second derivative filter SDEF in the ISEF technique. It uses the zero-crossing approach during obtaining edge detection. The SDEF provides the edge guided with higher precise edge localization [90]. From the observation, the edge detected by SDEF has a wider contour. To increase the precision localization and decrease the error detection rate. This study has proposed sharper edge detection by subtracting the different edges of initial guess with the edge of current estimation such as in (13).

$$\nabla f = (f - f_t) * ISEF - (f_t) * ISEF \tag{13}$$

This output of this difference provides a thinner and sharper edge detection. As a result, this estimator could determine the HR much accurately and faster than previous methods such result in the next section. Furthermore, to increase the robustness and computational efficiency, this technique collaborates with the Lorentzian norm, such as shown in (14).

$$f_{t+1} = f_t + \frac{1}{N} \rho_{lor} r^t + \tau \psi_{lor} [(f - f_t) * ISEF - (f_t) * ISEF] \tag{14}$$

The Lorentzian norm function ρ_{lor} is used to improve the error residual computation and the Lorentzian influence function ψ_{lor} increases the gradient detection value. While the threshold level T in the Lorentzian norm since $T > 1$ and it allows rapid correction in the residual error of the estimation. This condition catalyzes the estimator to reach the local minimum faster. Besides that, while the threshold level of the Lorentzian influence function $T_g > 1$, the level of gradient detected was increasing, and the estimator

capable to preserve many possible of the edge's information for each iteration. This proposed technique's process flow can be illustrated in Figure 3.

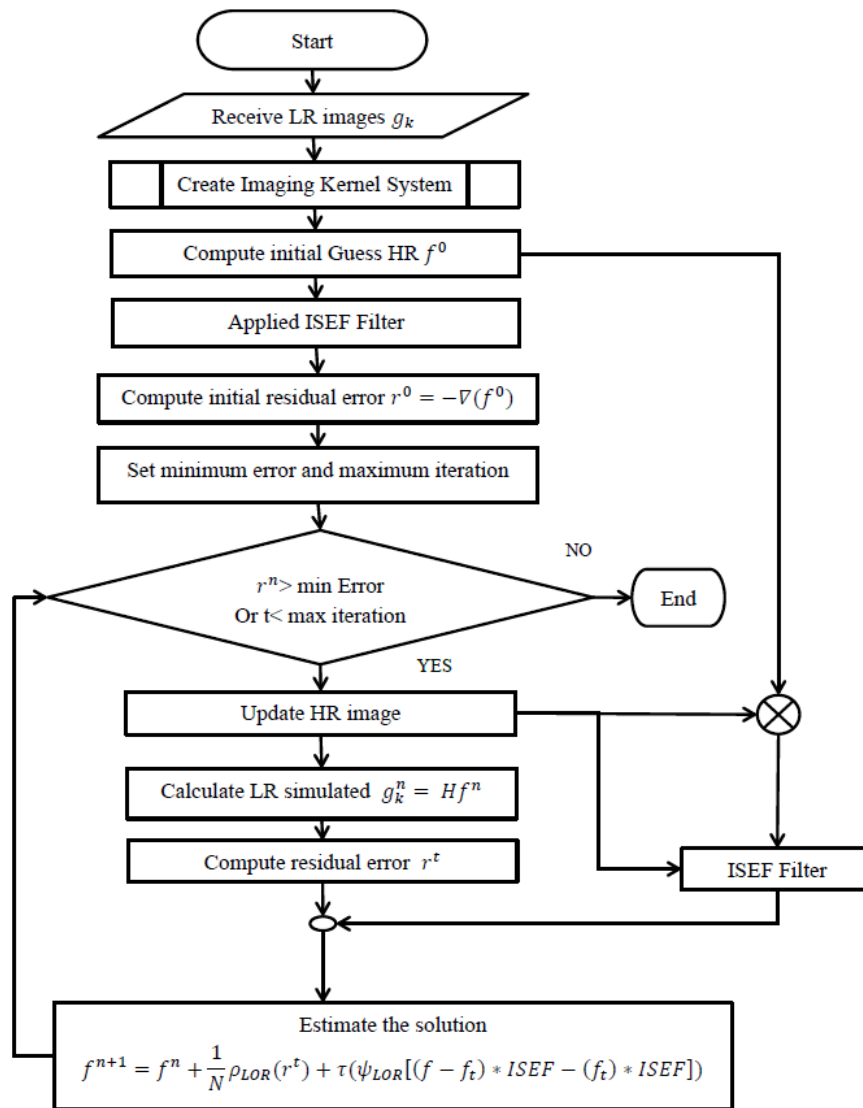


Figure 3. The IBP with Lorentzian ISEF regulator process flow

4. RESULT

The results of monitoring are shown in Tables 1 and 2, respectively. This section presents the discussion on experimental results have obtained by several techniques has explained before and including the proposed IBP with edge enhancement technique. The MATLAB platform is used as an experiment simulator in these experiments. Aside from that, these tests employ a regular image from the ISI and DESCAI databases, with a resolution of 256x256 pixels.

The initial procedure of this experiment creates a sequence of four LR images obtained from the image database. Each of the LR images created must have shifted from the original image by a pixel in the vertical direction. After that, they have applied the effect of camera PSF. The effect involves the process of blurry and decimation operation. This shifted LR image was then convoluted with a 3x3 Gaussian low pass filter with a standard deviation of 3. In each direction, the image was down sampled by a factor of two. As a result, four LR images are created using the same technique with varying motion vectors in vertical and horizontal dimensions. The PSNR magnitude is used to evaluate the suggested technique's performance. In addition, the cost computation complexity indicator is determined by the number of iterations required to complete the HR calculation.

4.1. Situation 1: The performance of the proposed technique with the variation of the input image

Table 1 reveals that the proposed LSISEF regulator methodology is responsible for the majority of the PSNR results. This means the proposed technique provides a better edge enhancement technique compared to other techniques. By looking at the average results, the LSISEF provides an improvement of about 2.12 dB from the conventional IBP technique. The key to improvement depends on the feature of the edge detector that provides a high localization precision, high rate detection, and small error rate detection. This positive change is illustrated in Figure 4 that provided a comparison output with the proposed technique which Figure 4(a) illustrates an input LR image and Figure 4(b) represents output HR produced by IBP and Figure 4(c) shows the proposed IBP with LSISEF technique output. Meanwhile, Figure 5 illustrates the overall output HR image from various techniques, such as Figure 5(a) represents the output of combination IBP with Canny method and Figure 5(b) shows the output by using patel method. In addition, Figure 5(c) represents the output of the cheref method and Figure 5(d) illustrates the output of the proposed technique which combined the IBP and LSISEF technique.

Table 1. Measurement of PSNR for IBP edge enhancement

	IBP	The IBP technique with			LSISEF
		Canny	Patel	Cheref	
LENA	27.730	28.018	28.651	28.034	28.990
CAMERAMAN	26.477	26.758	27.220	27.319	27.321
MANDRILL	23.284	23.336	23.464	23.486	23.494
PEPPER	25.941	26.391	27.956	29.023	30.676
CLOWN	24.560	25.067	26.673	27.932	29.868
JETPLANE	26.020	26.353	27.177	27.571	27.707
BRAIN	28.041	28.699	30.131	31.319	32.681
SHIP	28.923	29.188	29.494	29.714	29.609
USAF	22.670	22.656	22.183	22.624	22.783
BRIDGE	23.982	24.178	24.648	24.824	25.763
Average	25.763	26.064	26.760	27.185	27.889

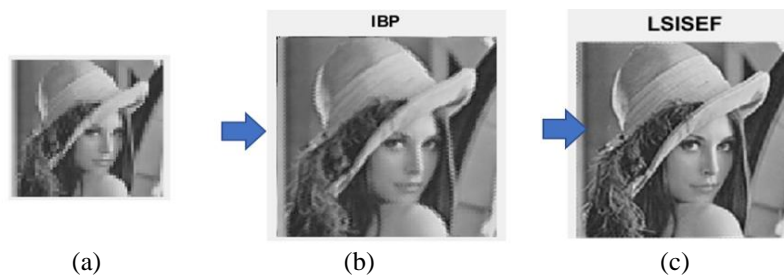


Figure 4. Comparison output with the proposed technique (a) input LR image, (b) HR image of IBP technique, and (c) HR image LSISEF (proposed)

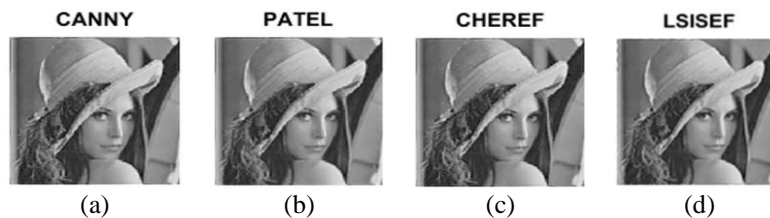


Figure 5. Overall output HR image (a) IBP+canny, (b) patel method, (c) cheref method, and (d) IBP+LSISEF (proposed)

The LSISEF edge detector has higher localization precision than the other edge detector, therefore in most cases of the image, the proposed ISEF technique gives better performance. The Lorentzian norm function and influence function can increase the level of edge detection, thus improves the correction task during estimation. The saturation level in the Lorentzian function is set equal to 1.5, consequence the norm function and influence function of the Lorentzian act as a weight of residual error and gradient detected,

respectively. This process increases the amount of gradient and relights the edge of the image. As a result, while our proposed methodology is capable of preserving high information detail losses and producing a finer output image with good performance, it has difficulties handling crucial images such as those with a lot of high-frequency information. The Mandrill image, for example, has a lot of high-frequency data, such as hair surrounding the Mandrill face. When the LSISEF detector simply traced the image's edges in the horizontal and vertical directions, this disadvantage arose. As a result, this detector failed to offer details of high-frequency information in some directions.

On the other hand, in some circumstances, Cheref's methodology also delivers the highest quality. This approach delivers the best quality, with a gain of roughly 1.42 decibels. This method worked effectively when dealing with challenging photos like Mandrill and USAF pictures. Cheref's anisotropic diffusion can offer edge detail in a variety of orientations (north, south, west, east). As a result, this method can provide detailed edge information as well as a promising result in a challenging image. Furthermore, this edge detector has a low sensitivity to reduction edges and has a good rate of detection. Thus, this technique is among the best edge enhancement technique. However, this technique has less localization compared to the LSISEF technique.

Shreyas [94] have proposed the combination of the IBP technique with the ISEF edge detector. As aforementioned before, the ISEF provides high precision in edge localization and less response to the error. Therefore, it can increase the quality image up to 0.997 dB in average value. Unfortunately, this edge detection only coverage about vertical and horizontal directions, because of this limitation the improvement only preserves the edge in limits directions. At the same time, the edge detected by this technique is not tiny enough and it may invite small error detection. Consequently, the Patel works failed to provide a higher improvement on the IBP reconstruction technique.

The Canny method is Gaussian based technique, and the result showed this technique only provides just a little improvement [76]. This technique has less error detection since it provides a very sharp edge image detected. However, this filter has disadvantages in the sensitivity detection rate. When a Gaussian-based filter has a contradiction function between giving a smooth function and an accurate localization rate, this problem occurs. As result this technique only capable to increase about 0.301 dB and the lowest improvement compared with other edge enhancement techniques.

4.2. Situation 2: Blurry effect information unknown

The objectives of this experiment are to evaluate the robustness of the IBP edge enhancement technique toward the blind blurry effects. This experiment assumes the image registration stage is failed to predict blur effect information accurately from the degraded input image. To imitate the real situation, this experiment uses injecting the unknown level of Gaussian blur effect to multiple input LR images. The blurry effect has 5x5 matrix size is used with varying values of sigma from 0.5, 1.0, 1.5, 2.0, 2.5, and 3.0. To perform the de-blurring process, the kernel system is required to pick a random sigma value. Thus, this experiment uses the small sigma value is 0.5 as the kernel system random default sigma value. This experiment measuring the quality and cost computation of the IBP with the edge enhancement.

Generally, the collection of the result in Table 2 shows that the proposed techniques capable to manage the blind blurring condition. Specifically, this technique successfully recovers the lost information due to the effects of low to high blur levels applied to the input image. The larger standard deviation value of blur effects may cause a lot of high-frequency information to become attenuated and lost. In addition, the previous IBP method has lacked determination on preserving the losses. Thus, the IBP failed to estimate the HR image accurately. The result shows the IBP method capable to provide the highest quality output if the blurry information used is the same as a blurry amount in the degraded input image. However, the performance of IBP going to drop if blurry information applied diverts far from an actual blurry amount in the LR image. For example, in the case of the standard deviation of Gaussian blur equal 0.5 is applied to the input image and the IBP kernel system. As a result, this technique produced a quality image of 33.594 dB. However, the quality of the output image decreased to 22.187 dB when increases the amount of blurring up to 3 which is the standard deviation value that has deviated far from the system expected.

This IBP weakness can improve by implementing the edge enhancement technique. The result in Table 2 shows, the LSISEF technique produces the highest quality images compared to other techniques. In average result, this combination gives improvement up to 3.182 dB compared to conventional IBP. Besides that, the average result of the SISEF method is capable to increase the quality image by about 3.073 dB better than the ordinary IBP technique. This result also conveyed the ISEF based is capable to provide good edge detection in highly blurry situations. In addition, the sharpening technique on the proposed technique also contributed to provide good results. However, the quality performance is slightly decreased from the Cheref method. This condition happens, when the clipper function tends to remove some amount of high-frequency information in the Anisotropic Diffusion. As a result, this technique slightly is degraded the performance quality of the Cheref method by about 0.539 dB.

However, the edge detector of Gaussian filter-based techniques such as Canny regulators failed to preserve the highly blurred edge image. This technique has a less rate of sensitive detection of the possible edge compared to anisotropic diffusion and ISEF. Therefore, during the sigma blur=3.0, most of the techniques have a weakness to predict the HR image and difficulty in recovering the lost information at the same time. Besides that, the ISEF-based edge enhancement method provides a solution to solve this difficulty. Therefore, the proposed technique and technique proposed by Patel give a promising result during handling the effect of highly blurring.

In addition, this technique successfully provides the highest quality PSNR whenever the other technique failed to do so. This experiment proves the LSISEF can resist the condition of the highly blurred image since this image lost much high-frequency information. However, the edge detector of the Gaussian filter-based technique failed to preserve the weakest edge image. Therefore, most of them not efficient during handling the highest blur image. Moreover, during the standard deviation blur is 3, most of the technique has a disadvantage to predicting the HR image and coincide difficulty in recovering the lost information. However, the LSISEF based edge enhancement method has a solution to solve this difficulty. Therefore, the proposed technique and technique proposed by Patel give a trusty result during the highly blurry effect given. In the future, it is planning to utilize this LSISEF method to improve the effectiveness of quality threshold ARTMAP [95], [96] in pattern recognition problems. In addition, further investigation will be done to increase the performance of the moment invariant technique [97] for the feature extraction process with the use of the LSISEF technique

Table 2. The performance comparison of the combination IBP with edge enhancement toward the blind blurry effect

	IBP	The IBP technique with			
		Canny	Patel	Cheref	LSISEF
Sigma = 0.5	33.594	33.592	32.528	33.151	33.046
Sigma = 1.0	27.436	27.436	28.613	27.400	28.711
Sigma = 1.5	24.611	24.611	27.919	25.281	27.982
Sigma =2.0	23.24	23.240	27.699	24.415	27.751
Sigma = 2.5	22.561	22.561	27.600	24.009	27.648
Sigma = 3.0	22.187	22.187	27.548	23.789	27.594
Average	25.60483	25.6045	28.65117	26.34083	28.78867

5. CONCLUSION

This study proposes using the Lorentzian Sharp ISEF (LSISEF) regularization as a robust edge enhancement to improve the IBP reconstruction technique problem. In the past, the IBP reconstruction methodology was plagued with ringing artifacts, necessitating a high number of iterations to complete the estimation. Furthermore, due to fuzzy effects, this approach loses the potential to preserve lost high-frequency information. As a result, in this study, the Lorentzian Sharp ISEF regulator was designed to provide a remedy to the IBP reconstruction defects by providing precise edge enhancement with light cost computation. As a result, this proposed technique provided 2.12 dB better PSNR compared to the conventional IBP technique after examined with various input images. Additionally, this proposed technique provided 3.182 dB PSNR better than conventional IBP in a vary of blurry PSF functions. This result came about as a result of the method's high precision localization and low error rate detection when used as an edge detector. These benefits enable the estimator to calculate the corrective process more precisely and quickly. At the same time, the Lorentzian norm and influence function increase the quality residual computation and gradient detection, respectively.

ACKNOWLEDGEMENTS

The author would like to acknowledge the support from the Fundamental Research Grant Scheme (FRGS) under a grant number of RACER/1/2019/ICT02/UNIMAP//1 from the Ministry of Higher Education Malaysia. The author would like to express gratitude to the Ministry of Higher Education Malaysia and University Malaysia Perlis for the facilities provided in this work.

REFERENCES




- [1] X. Niu, "An overview of image super-resolution reconstruction algorithm," in *2018 11th International Symposium on Computational Intelligence and Design (ISCID)*, Dec. 2018, vol. 2, pp. 16–18, doi: 10.1109/ISCID.2018.10105.
- [2] L. Morera-Delfín, R. Pinto-Elías, and H.-J. Ochoa-Domínguez, "Overview of super-resolution techniques," in *Advanced Topics*

- on *Computer Vision, Control and Robotics in Mechatronics*, Cham: Springer International Publishing, 2018, pp. 101–127.
- [3] S. Anwar, S. Khan, and N. Barnes, “A deep journey into super-resolution,” *ACM Computing Surveys*, vol. 53, no. 3, pp. 1–34, May 2021, doi: 10.1145/3390462.
- [4] Y.-Q. Y. Q. Tang, H. Pan, Y.-P. Y. P. Zhu, and X. D. X.-D. Li, “A survey of image super-resolution reconstruction,” *Tien Tzu Hsueh Pao/Acta Electronica Sinica*, vol. 48, no. 7, pp. 1407–1420, 2020, doi: 10.3969/j.issn.0372-2112.2020.07.022.
- [5] T. Yao, Y. Luo, Y. Chen, D. Yang, and L. Zhao, “Single-image super-resolution: a survey,” in *Lecture Notes in Electrical Engineering*, vol. 516, 2020, pp. 119–125.
- [6] Q. Xu and Y. Zheng, “A survey of image super resolution based on CNN,” in *Lecture Notes of the Institute for Computer Sciences, Social-Informatics and Telecommunications Engineering, LNICST*, vol. 322 LNICST, 2020, pp. 184–199.
- [7] J. Parekh, P. Turakhia, H. Bhinderwala, and S. N. Dhage, “A survey of image enhancement and object detection methods,” in *Advances in Intelligent Systems and Computing*, vol. 1158, 2021, pp. 1035–1047.
- [8] A. S. Chernyavskiy, “Super-resolution: 2. Machine learning-based approach,” *Signals and Communication Technology*, pp. 35–58, 2021.
- [9] Z. Liu *et al.*, “A survey on applications of deep learning in microscopy image analysis,” *Computers in Biology and Medicine*, vol. 134, p. 104523, Jul. 2021, doi: 10.1016/j.combiomed.2021.104523.
- [10] K. Nguyen, C. Fookes, S. Sridharan, M. Tistarelli, and M. Nixon, “Super-resolution for biometrics: A comprehensive survey,” *Pattern Recognition*, vol. 78, pp. 23–42, Jun. 2018, doi: 10.1016/j.patcog.2018.01.002.
- [11] S. S. Rajput, K. V. Arya, V. Singh, and V. K. Bohat, “Face hallucination techniques: a survey,” in *2018 Conference on Information and Communication Technology (CICT)*, Oct. 2018, pp. 1–6, doi: 10.1109/INCOMTECH.2018.8722416.
- [12] N. P. Del Gallego and J. Ilaó, “Improving multiple-image super-resolution for mobile devices through image alignment selection,” *Journal of WSCG*, vol. 26, no. 2, pp. 122–131, 2018, doi: 10.24132/JWSCG.2018.26.2.7.
- [13] V. K. Ha *et al.*, “Deep learning based single image super-resolution: a survey,” *International Journal of Automation and Computing*, vol. 16, no. 4, pp. 413–426, Aug. 2019, doi: 10.1007/s11633-019-1183-x.
- [14] W. Yang, X. Zhang, Y. Tian, W. Wang, J.-H. Xue, and Q. Liao, “Deep learning for single image super-resolution: a brief review,” *IEEE Transactions on Multimedia*, vol. 21, no. 12, pp. 3106–3121, Dec. 2019, doi: 10.1109/TMM.2019.2919431.
- [15] J. Yang, Z. Jiang, X. Ye, and K. Li, “Depth super-resolution with color guidance: a review,” in *Advances in Computer Vision and Pattern Recognition*, 2019, pp. 51–65.
- [16] X. Li, Y. Wu, W. Zhang, R. Wang, and F. Hou, “Deep learning methods in real-time image super-resolution: a survey,” *Journal of Real-Time Image Processing*, vol. 17, no. 6, pp. 1885–1909, Dec. 2020, doi: 10.1007/s11554-019-00925-3.
- [17] Z. Yang, P. Shi, and D. Pan, “A survey of super-resolution based on deep learning,” in *2020 International Conference on Culture-oriented Science and Technology (ICCST)*, Oct. 2020, pp. 514–518, doi: 10.1109/ICCST50977.2020.00106.
- [18] H. Shen, B. Hou, Z. Wen, and L. Jiao, “Structural-correlated self-examples based superresolution of single remote sensing image,” *IEEE Journal of Selected Topics in Applied Earth Observations and Remote Sensing*, vol. 11, no. 9, pp. 3209–3223, Sep. 2018, doi: 10.1109/JSTARS.2018.2847450.
- [19] J. Zhao, T. Sun, and F. Cao, “Image super-resolution via adaptive sparse representation and self-learning,” *IET Computer Vision*, vol. 12, no. 5, pp. 753–761, Aug. 2018, doi: 10.1049/iet-cvi.2017.0153.
- [20] A. Urikura, T. Yoshida, Y. Nakaya, E. Nishimaru, T. Hara, and M. Endo, “Deep learning-based reconstruction in ultra-high-resolution computed tomography: Can image noise caused by high definition detector and the miniaturization of matrix element size be improved?,” *Physica Medica*, vol. 81, pp. 121–129, Jan. 2021, doi: 10.1016/j.ejmp.2020.12.006.
- [21] T. Gomi, “Development of a novel algorithm to improve image quality in chest digital tomosynthesis using convolutional neural network with super-resolution,” in *Medical Imaging 2021: Physics of Medical Imaging*, Feb. 2021, vol. 11595, p. 177, doi: 10.1117/12.2581917.
- [22] H. Chen, X. Zhang, Y. Liu, and Q. Zeng, “Generative adversarial networks capabilities for super-resolution reconstruction of weather radar echo images,” *Atmosphere*, vol. 10, no. 9, p. 555, Sep. 2019, doi: 10.3390/atmos10090555.
- [23] M. Irfan *et al.*, “Single image super resolution technique: an extension to true color images,” *Symmetry*, vol. 11, no. 4, p. 464, Apr. 2019, doi: 10.3390/sym11040464.
- [24] K. Malczewski, “Motion artifacts free image resolution enhancement exploiting image priors,” in *2017 International Conference on Systems, Signals and Image Processing (IWSSIP)*, May 2017, pp. 1–4, doi: 10.1109/IWSSIP.2017.7965576.
- [25] Y. Cheref and D. Yousfi, “Image reconstruction with better edge enhancement using super resolution algorithm,” in *2014 International Conference on Multimedia Computing and Systems (ICMCS)*, Apr. 2014, pp. 283–288, doi: 10.1109/ICMCS.2014.6911234.
- [26] H. Zhu, X. Tang, J. Xie, W. Song, F. Mo, and X. Gao, “Spatio-temporal super-resolution reconstruction of remote-sensing images based on adaptive multi-scale detail enhancement,” *Sensors*, vol. 18, no. 2, p. 498, Feb. 2018, doi: 10.3390/s18020498.
- [27] M. Hao-yu, X. Zhi-hai, F. Hua-jun, L. Qi, and C. Yue-ting, “Image super-resolution based on tiny recurrent convolutional neural network,” *Acta Photonica Sinica*, vol. 47, no. 4, p. 410004, 2018, doi: 10.3788/gzxb20184704.0410004.
- [28] X. Li, L. Li, and Q.-H. Wang, “Wavelet-based iterative perfect reconstruction in computational integral imaging,” *Journal of the Optical Society of America A*, vol. 35, no. 7, p. 1212, Jul. 2018, doi: 10.1364/JOSAA.35.001212.
- [29] J. Zhao, Q. Yuan, J. Qin, X. Yang, and Z. Chen, “Single image super-resolution reconstruction using multiple dictionaries and improved iterative back-projection,” *Optoelectronics Letters*, vol. 15, no. 2, pp. 156–160, Mar. 2019, doi: 10.1007/s11801-019-8138-x.
- [30] L. J. Oostveen, K. L. Boedeker, M. Brink, M. Prokop, F. de Lange, and I. Sechopoulos, “Physical evaluation of an ultra-high-resolution CT scanner,” *European Radiology*, vol. 30, no. 5, pp. 2552–2560, May 2020, doi: 10.1007/s00330-019-06635-5.
- [31] X. Yang, F. Li, L. Xin, X. Lu, M. Lu, and N. Zhang, “An improved mapping with super-resolved multispectral images for geostationary satellites,” *Remote Sensing*, vol. 12, no. 3, p. 466, Feb. 2020, doi: 10.3390/rs12030466.
- [32] J.-S. Yoo and J.-O. Kim, “Noise-robust iterative back-projection,” *IEEE Transactions on Image Processing*, vol. 29, pp. 1219–1232, 2020, doi: 10.1109/TIP.2019.2940414.
- [33] S. J. Lakshmi and P. Deepa, “Image SR-based NLM and DCNN improved IBP with cubic B-spline,” *The Imaging Science Journal*, vol. 68, no. 3, pp. 129–140, Apr. 2020, doi: 10.1080/13682199.2020.1757294.
- [34] S. Jamaludin, N. Zainal, and W. M. D. W. Zaki, “Deblurring of noisy iris images in iris recognition,” *Bulletin of Electrical Engineering and Informatics*, vol. 10, no. 1, pp. 156–159, Feb. 2021, doi: 10.11591/eei.v10i1.2467.
- [35] Q. Yang, J. Lou, S. Liu, and A. Diao, “Super resolution imaging needs better registration for better quality results,” *Bulletin of Electrical Engineering and Informatics*, vol. 1, no. 1, pp. 43–50, Mar. 2012, doi: 10.12928/EEL.v1i1.30.
- [36] W. Dong, P. Wang, W. Yin, G. Shi, F. Wu, and X. Lu, “Denosing Prior Driven Deep Neural Network for Image Restoration,” *IEEE Transactions on Pattern Analysis and Machine Intelligence*, vol. 41, no. 10, pp. 2305–2318, Oct. 2019, doi: 10.1109/TPAMI.2018.2873610.




- [37] X. Liao, K. Bai, Q. Zhang, X. Jia, S. Liu, and J. Zhan, "Image super-resolution based on sparse coding with multi-class dictionaries," *Computing and Informatics*, vol. 38, no. 6, pp. 1301–1319, 2019, doi: 10.31577/cai.2019.5.1301.
- [38] R. H. Jagdale and S. K. Shah, "Super resolution reconstruction of low resolution video using sparse technique," in *2019 5th International Conference On Computing, Communication, Control And Automation (ICCUBEA)*, Sep. 2019, pp. 1–5, doi: 10.1109/ICCUBEA47591.2019.9129328.
- [39] C. Cruz, R. Mehta, V. Katkovnik, and K. O. Egiazarian, "Single image super-resolution based on wiener filter in similarity domain," *IEEE Transactions on Image Processing*, vol. 27, no. 3, pp. 1376–1389, Mar. 2018, doi: 10.1109/TIP.2017.2779265.
- [40] W.-T. Lu, C.-W. Lin, C.-H. Kuo, and Y.-C. Tung, "Image super-resolution based on error compensation with convolutional neural network," in *2017 Asia-Pacific Signal and Information Processing Association Annual Summit and Conference (APSIPA ASC)*, Dec. 2017, vol. 2018-Febru, pp. 1160–1163, doi: 10.1109/APSIPA.2017.8282203.
- [41] M. Irani and S. Peleg, "Super resolution from image sequences," in *[1990] Proceedings. 10th International Conference on Pattern Recognition*, 1990, vol. ii, pp. 115–120, doi: 10.1109/ICPR.1990.119340.
- [42] T. Ma and W. Tian, "Arbitrary back-projection networks for image super-resolution," *International Journal of Computational Intelligence and Applications*, vol. 19, no. 04, p. 2050026, Dec. 2020, doi: 10.1142/S1469026820500261.
- [43] W. Dianwei, H. Yuanjie, L. Ying, X. Yongjun, and S. Haijun, "Super-resolution reconstruction of license plate image based on gradual back-projection network," *Laser and Optoelectronics Progress*, vol. 57, no. 16, p. 161002, 2020, doi: 10.3788/LOP57.161002.
- [44] L. Zhang, M. Li, and X. Deng, "Image super-resolution using multi-dictionary sparse representation," in *Proceedings of the 5th International Conference on Multimedia and Image Processing*, Jan. 2020, pp. 61–66, doi: 10.1145/3381271.3381294.
- [45] A. R. A. Nazren, R. Ngadiran, and S. N. Yaakob, "Edge enhancement of IBP reconstruction by using sharp infinite symmetrical exponential filter," *Indonesian Journal of Electrical Engineering and Computer Science*, vol. 14, no. 1, pp. 258–266, Apr. 2019, doi: 10.11591/ijeecs.v14.i1.pp258-266.
- [46] M. Irani and S. Peleg, "Motion analysis for image enhancement: resolution, occlusion, and transparency," *Journal of Visual Communication and Image Representation*, vol. 4, no. 4, pp. 324–335, Dec. 1993, doi: 10.1006/jvci.1993.1030.
- [47] S. Kiatpapan, T. Yamaguchi, and M. Ikehara, "Super-resolution based on back-projection of interpolated image," in *2019 International Conference on Advanced Technologies for Communications (ATC)*, Oct. 2019, vol. 2019-October, pp. 302–307, doi: 10.1109/ATC.2019.8924492.
- [48] M. Irani and S. Peleg, "Improving resolution by image registration," *CVGIP: Graphical Models and Image Processing*, vol. 53, no. 3, pp. 231–239, May 1991, doi: 10.1016/1049-9652(91)90045-L.
- [49] B. M. Ngocho and E. Mwangi, "An iterative back-projection technique for single image super resolution with natural texture preservation," in *Emerging Trends in Electrical, Electronic and Communications Engineering: Proceedings of the First International Conference on Electrical, Electronic and Communications Engineering (ELECOM 2016)*, Bagatelle, Mauritius, November 25 -27, 2016, P. Fleming, N. Vyas, S. Sanei, and K. Deb, Eds. Cham: Springer International Publishing, 2017, pp. 210–219.
- [50] J. Zheng, J. A. Fessler, and H.-P. Chan, "Segmented separable footprint projector for digital breast tomosynthesis and its application for subpixel reconstruction," *Medical Physics*, vol. 44, no. 3, pp. 986–1001, Mar. 2017, doi: 10.1002/mp.12092.
- [51] C. A. Ayanda, S. Nizam Bin Yaakob, and M. Nawir, "Uniqueness of iterative back projection in super resolution techniques," in *2016 3rd International Conference on Electronic Design (ICED)*, Aug. 2016, pp. 501–506, doi: 10.1109/ICED.2016.7804696.
- [52] Y. Li, J. Li, T. Wang, M. Lian, and S. Luo, "Micro-CT imaging of super-resolution MBIR algorithm based on sub-pixel displacement," in *Medical Imaging 2020: Physics of Medical Imaging*, Mar. 2020, vol. 11312, p. 131, doi: 10.1117/12.2549418.
- [53] F. Geng, H. Liu, Q. Guo, and Y. Yin, "Variational optical flow estimation based super-resolution reconstruction for lung 4D-CT image," *Jisuanji Yanjiu yu Fazhan/Computer Research and Development*, vol. 54, no. 8, pp. 1703–1712, 2017.
- [54] L. Wu, Z. Li, Y. Zhang, C. Wen, and S. Zhang, "Single text image super-resolution based on edge-compensated autoregressive model," in *2017 International Conference on the Frontiers and Advances in Data Science (FADS)*, Oct. 2017, vol. 2018-Janua, pp. 155–158, doi: 10.1109/FADS.2017.8253218.
- [55] A. R. A. Nazren, S. N. Yaakob, R. Ngadiran, M. B. Hisham, and N. M. Wafi, "Improving iterative back projection super resolution model via anisotropic diffusion edge enhancement," in *2016 International Conference on Robotics, Automation and Sciences (ICORAS)*, Nov. 2016, pp. 1–4, doi: 10.1109/ICORAS.2016.7872612.
- [56] H. Zheng *et al.*, "Multi-Contrast Brain MRI Image Super-Resolution with Gradient-Guided Edge Enhancement," *IEEE Access*, vol. 6, pp. 57856–57867, 2018, doi: 10.1109/ACCESS.2018.2873484.
- [57] H. Liu, Y. Lin, B. Ibragimov, and C. Zhang, "Low dose 4D-CT super-resolution reconstruction via inter-plane motion estimation based on optical flow," *Biomedical Signal Processing and Control*, vol. 62, p. 102085, Sep. 2020, doi: 10.1016/j.bspc.2020.102085.
- [58] R. Nayak and D. Patra, "An edge preserving IBP based super resolution image reconstruction using P-spline and MuCSO-QPSO algorithm," *Microsystem Technologies*, vol. 23, no. 3, pp. 553–569, Mar. 2017, doi: 10.1007/s00542-016-2972-6.
- [59] R. Nayak and D. Patra, "Enhanced iterative back-projection based super-resolution reconstruction of digital images," *Arabian Journal for Science and Engineering*, vol. 43, no. 12, pp. 7521–7547, Dec. 2018, doi: 10.1007/s13369-018-3150-1.
- [60] T. Tirer and R. Giryes, "Back-Projection Based Fidelity Term for Ill-Posed Linear Inverse Problems," *IEEE Transactions on Image Processing*, vol. 29, pp. 6164–6179, 2020, doi: 10.1109/TIP.2020.2988779.
- [61] M.-C. Chiang and T. E. Boult, "Efficient image warping and super-resolution," in *Proceedings Third IEEE Workshop on Applications of Computer Vision. WACV'96*, 1996, pp. 56–61, doi: 10.1109/ACV.1996.572000.
- [62] B. Cohen and I. Dinstein, "Polyphase back-projection filtering for image resolution enhancement," *IEE Proceedings-Vision, Image, and Signal Processing*, vol. 147, no. 4, p. 318, 2000, doi: 10.1049/ip-vis:20000333.
- [63] H. Kim, J.-H. Jang, and K.-S. Hong, "Edge-enhancing super-resolution using anisotropic diffusion," *Proceedings 2001 International Conference on Image Processing (Cat. No.01CH37205)*, vol. 2, IEEE, pp. 130–133, 2001, doi: 10.1109/ICIP.2001.958068.
- [64] N. K. Bose, S. Lertrattanapanich, and J. Koo, "Advances in superresolution using L-curve," in *ISCAS 2001. The 2001 IEEE International Symposium on Circuits and Systems (Cat. No.01CH37196)*, 2001, vol. 2, pp. 433–436, doi: 10.1109/ISCAS.2001.921100.
- [65] D. Rajan and S. Chaudhuri, "Data fusion techniques for super-resolution imaging," *Information Fusion*, vol. 3, no. 1, pp. 25–38, Mar. 2002, doi: 10.1016/S1566-2535(01)00044-6.
- [66] J. Sun, N.-N. Zheng, H. Tao, and H.-Y. Shum, "Image hallucination with primal sketch priors," in *2003 IEEE Computer Society Conference on Computer Vision and Pattern Recognition, 2003. Proceedings*, 2003, vol. 2, pp. II-729–36, doi: 10.1109/CVPR.2003.1211539.

- [67] D. Rajan and S. Chaudhuri, "Simultaneous estimation of super-resolved scene and depth map from low resolution defocused observations," *IEEE Transactions on Pattern Analysis and Machine Intelligence*, vol. 25, no. 9, pp. 1102–1117, Sep. 2003, doi: 10.1109/TPAMI.2003.1227986.
- [68] S. H. Or, Y. K. Yu, K. H. Wong, and M. M. Yuen Chang, "Resolution improvement from stereo images with 3D pose differences," in *2006 International Conference on Image Processing*, Oct. 2006, pp. 1733–1736, doi: 10.1109/ICIP.2006.312716.
- [69] S. Dai, M. Han, Y. Wu, and Y. Gong, "Bilateral back-projection for single image super resolution," in *Multimedia and Expo, 2007 IEEE International Conference on*, Jul. 2007, pp. 1039–1042, doi: 10.1109/ICME.2007.4284831.
- [70] W. Dong, L. Zhang, G. Shi, and X. Wu, "Nonlocal back-projection for adaptive image enlargement," in *2009 16th IEEE International Conference on Image Processing (ICIP)*, Nov. 2009, pp. 349–352, doi: 10.1109/ICIP.2009.5414423.
- [71] E. Faramarzi, V. R. Bhakta, D. Rajan, and M. P. Christensen, "Super resolution results in PANOPTES, an adaptive multi-aperture folded architecture," in *2010 IEEE International Conference on Image Processing*, Sep. 2010, pp. 2833–2836, doi: 10.1109/ICIP.2010.5652102.
- [72] Z. Yan, Y. Lu, and H. Yan, "Reducing the spiral CT slice thickness using super resolution," *2010 IEEE International Conference on Image Processing*, pp. 593–596, 2010, doi: 10.1109/ICIP.2010.5652144.
- [73] F. Qin, "An improved super resolution reconstruction method based on initial value estimation," in *2010 3rd International Congress on Image and Signal Processing*, Oct. 2010, pp. 826–829, doi: 10.1109/CISP.2010.5646854.
- [74] X. Liang and Z. Gan, "Improved non-local iterative back-projection method for image super-resolution," in *2011 Sixth International Conference on Image and Graphics*, Aug. 2011, pp. 176–181, doi: 10.1109/ICIG.2011.108.
- [75] T. Bengtsson, I. Y.-H. Gu, M. Viberg, and K. Lindstrom, "Regularized optimization for joint super-resolution and high dynamic range image reconstruction in a perceptually uniform domain," in *2012 IEEE International Conference on Acoustics, Speech and Signal Processing (ICASSP)*, Mar. 2012, pp. 1097–1100, doi: 10.1109/ICASSP.2012.6288078.
- [76] M. N. Bareja and C. K. Modi, "An effective iterative back projection based single image super resolution approach," in *2012 International Conference on Communication Systems and Network Technologies*, May 2012, pp. 95–99, doi: 10.1109/CSNT.2012.30.
- [77] R. Nayak, S. Monalisa, and D. Patra, "Spatial super resolution based image reconstruction using HIBP," in *2013 Annual IEEE India Conference (INDICON)*, Dec. 2013, pp. 1–6, doi: 10.1109/INDICON.2013.6726146.
- [78] P. Rasti, H. Demirel, and G. Anbarjafari, "Image resolution enhancement by using interpolation followed by iterative back projection," in *2013 21st Signal Processing and Communications Applications Conference (SIU)*, Apr. 2013, pp. 1–4, doi: 10.1109/SIU.2013.6531593.
- [79] B. Maiseli, O. Elisha, J. Mei, and H. Gao, "Edge preservation image enlargement and enhancement method based on the adaptive Perona-Malik non-linear diffusion model," *IET Image Processing*, vol. 8, no. 12, pp. 753–760, Dec. 2014, doi: 10.1049/iet-ipt.2014.0040.
- [80] A. Zomet, A. Rav-Acha, and S. Peleg, "Robust super-resolution," in *Proceedings of the 2001 IEEE Computer Society Conference on Computer Vision and Pattern Recognition. CVPR 2001*, 2001, vol. 1, pp. I-645–I-650, doi: 10.1109/CVPR.2001.990535.
- [81] S. Farsi, "A fast and robust framework for image fusion and enhancement," *Thesis*, p. 171, 2005.
- [82] S. Z. S. Hassen and M. I. Jahmeerbacus, *Emerging trends in electrical, electronic and communications engineering*, vol. 416, no. 1. Cham: Springer International Publishing, 2017.
- [83] V. Patanavijit and S. Jitapunkul, "A Lorentzian Bayesian approach for robust iterative multiframe super-resolution reconstruction with Lorentzian-tikhonov regularization," in *2006 International Symposium on Communications and Information Technologies*, Oct. 2006, pp. 1044–1049, doi: 10.1109/ISCIT.2006.339937.
- [84] M. V. W. Zibetti and J. Mayer, "Outlier Robust and Edge-Preserving Simultaneous Super-Resolution," in *2006 International Conference on Image Processing*, Oct. 2006, pp. 1741–1744, doi: 10.1109/ICIP.2006.312718.
- [85] V. Patanavijit and S. Jitapunkul, "A Lorentzian stochastic estimation for a robust iterative multiframe super-resolution reconstruction with lorentzian-tikhonov regularization," *EURASIP Journal on Advances in Signal Processing*, vol. 2007, no. 1, p. 34821, Dec. 2007, doi: 10.1155/2007/34821.
- [86] V. Patanavijit and S. Jitapunkul, "A robust iterative multiframe super-resolution reconstruction using a Bayesian approach with Lorentzian norm," in *2006 10th IEEE Singapore International Conference on Communication Systems*, 2006, pp. 1–5, doi: 10.1109/ICCS.2006.301414.
- [87] R. Lai, Y. Yang, H. Zhou, H. Qin, and B. Wang, "Total variation regularized iterative back-projection method for single frame image super resolution," in *2012 IEEE 11th International Conference on Signal Processing*, Oct. 2012, no. 2, pp. 931–934, doi: 10.1109/ICoSP.2012.6491732.
- [88] W. Feng and H. Lei, "Single-image super-resolution with total generalised variation and Shearlet regularisations," *IET Image Processing*, vol. 8, no. 12, pp. 833–845, Dec. 2014, doi: 10.1049/iet-ipt.2013.0503.
- [89] X. Yang, Y. Zhang, D. Zhou, and R. Yang, "An improved iterative back projection algorithm based on ringing artifacts suppression," *Neurocomputing*, vol. 162, pp. 171–179, Aug. 2015, doi: 10.1016/j.neucom.2015.03.055.
- [90] S. Castan, J. Zhao, and J. Shen, "New edge detection methods based on exponential filter," in *[1990] Proceedings. 10th International Conference on Pattern Recognition*, 1990, vol. i, no. X, pp. 709–711, doi: 10.1109/ICPR.1990.118199.
- [91] M. J. Black and G. Sapiro, "Edges as outliers: anisotropic smoothing using local image statistics," M. Nielsen, P. Johansen, O. F. Olsen, and J. Weickert, Eds. Berlin: Springer Berlin Heidelberg, 1999, pp. 259–270.
- [92] M. J. Black, G. Sapiro, D. H. Marimont, and D. Heeger, "Robust anisotropic diffusion," *IEEE Transactions on Image Processing*, vol. 7, no. 3, pp. 421–432, Mar. 1998, doi: 10.1109/83.661192.
- [93] M. J. Black, G. Sapiro, D. Marimont, and D. Heeger, "Robust anisotropic diffusion: Connections between robust statistics, line processing, and anisotropic diffusion," B. ter Haar Romeny, L. Florack, J. Koenderink, and M. Viergever, Eds. Berlin: Springer Berlin Heidelberg, 1997, pp. 323–326.
- [94] P. S. A. Patel Shreyas A., "Novel iterative back projection approach," *IOSR Journal of Computer Engineering*, vol. 11, no. 1, pp. 65–69, 2013, doi: 10.9790/0661-1116569.
- [95] S. N. Yaakob, C. P. Lim, and L. Jain, "A novel Euclidean quality threshold ARTMAP network and its application to pattern classification," *Neural Computing and Applications*, vol. 19, no. 2, pp. 227–236, Mar. 2010, doi: 10.1007/s00521-009-0293-8.
- [96] W. N. van Wieringen, "Lecture notes on ridge regression," pp. 0–30, Sep. 2015, arXiv:1509.09169.
- [97] S. N. Yaakob, P. Saad, and A. H. Abdullah, "Trademarks classification by moment invariant and FuzzyARTMAP," no. 1, pp. 117–122.




BIOGRAPHIES OF AUTHORS

Amir Nazren Abdul Rahim    was awarded the B. Engineering (Hons) in Computer Engineering from Universiti Malaysia Perlis (UniMAP), Malaysia. Then continue his studies Ph.D. degree in Computer Engineering from Universiti Malaysia Perlis (UniMAP), Malaysia. He can be reached through e-mail amirnazren@unimap.edu.my.






Shahrul Nizam Yaakob    obtained the B.Eng. in Electrical-Electronics (Hons) from University Teknologi Malaysia (UTM) and M.S. degrees by research in Computer Engineering from University Malaysia Perlis (UniMAP). He continued his Ph.D. degree in Computer System Engineering from University South Australia, Australia. He can be reached through e-mail shahrulnizam@unimap.edu.my.






Lee Yenfg Seng    received a B. Engineering (Hons) in Communication Engineering from Universiti Malaysia Perlis Malaysia (UniMAP). He obtained a Ph.D. degree in Communications from Universiti Malaysia Perlis (UniMAP), Perlis, Malaysia. He can be reached through e-mail yslee@unimap.edu.my.



Iszaidy Ismail    obtained the Bachelor of Science (Electronics and Electrical Engineering) from Sungkyunkwan University, Korea, and M.S. degrees by research in Computer Engineering from University Malaysia Perlis (UniMAP). He got awarded a Ph.D. degree in Computer Engineering from Universiti Malaysia Perlis (UniMAP), Malaysia. He can be reached through an e-mail iszaidy@unimap.edu.my.



Mohd Wafi Nasruddin    obtained the B. Engineering (Hons) in Computer Engineering from Universiti Malaysia Perlis (UniMAP), Malaysia, and M.S. degrees by research in Computer Engineering from University Malaysia Perlis (UniMAP). Then he was awarded a Ph.D. degree in Computer Engineering from Universiti Malaysia Perlis (UniMAP), Malaysia. He can be reached through an e-mail: wafi@unimap.edu.my.